Fine-tuning the functionality of reduced graphene oxide via bipolar electrochemistry in freestanding 2D reaction layers

Seyyed Mohsen Beladi-Mousavi, Gerardo Salinas, Nikolas Antonatos, Vlastimil Mazanek, Patrick Garrigue, Zdeněk Sofer, Alexander Kuhn

▶ **To cite this version:**

Seyyed Mohsen Beladi-Mousavi, Gerardo Salinas, Nikolas Antonatos, Vlastimil Mazanek, Patrick Garrigue, et al.. Fine-tuning the functionality of reduced graphene oxide via bipolar electrochemistry in freestanding 2D reaction layers. Carbon, 2022, 191, pp.439-447. ⟨10.1016/j.carbon.2022.02.010⟩. ⟨hal-03635847⟩

HAL Id: hal-03635847

https://hal.science/hal-03635847v1

Submitted on 25 Apr 2022

HAL is a multi-disciplinary open access archive for the deposit and dissemination of scientific research documents, whether they are published or not. The documents may come from teaching and research institutions in France or abroad, or from public or private research centers.

L'archive ouverte pluridisciplinaire **HAL**, est destinée au dépôt et à la diffusion de documents scientifiques de niveau recherche, publiés ou non, émanant des établissements d'enseignement et de recherche français ou étrangers, des laboratoires publics ou privés.

HAL Authorization

Fine-Tuning the Functionality of Reduced Graphene Oxide via Bipolar Electrochemistry in Freestanding 2D Reaction Layers

Seyyed Mohsen Beladi-Mousavi,[a] *Gerardo Salinas,*[a] *Nikolas Antonatos,*[b] *Vlastimil Mazanek,*[b] *Patrick Garrigue,*[a] *Zdeněk Sofer,*[b] *Alexander Kuhn*[a]*

[a] Univ. Bordeaux, CNRS, Bordeaux INP, ISM, UMR 5255, ENSCBP, 33607, Pessac, France
* Tel: +33 5 56 84 65 97 E-mail: kuhn@enscbp.fr (Alexander Kuhn)

[b] Department of Inorganic Chemistry, University of Chemistry and Technology Prague Technicka 5, 166 28 Prague 6, Czech Republic

Keywords: reduced graphene oxide, bipolar electrochemistry, energy storage, energy conversion, HER, wireless electrochemistry

Abstract

Graphene has unique characteristics that are appealing for energy-related applications such as ultra-lightweight and high surface-area/electrical-conductivity. However, generating functional graphene sheets is still a very challenging task. Here, a novel approach based on an original bipolar electrochemistry set-up, using a quasi-2D reaction layer, is suggested, which allows a precise control of dispersibility and conductivity of graphene sheets. In this system, a freestanding 2D layer of aqueous solution, containing 2D graphene oxide (GO) sheets, is placed between two platinum feeder electrodes, which are used to apply an electric field. As a result, the GO sheets experience a sufficiently high polarization to cause their transformation into reduced GO (rGO). The degree of reduction can be readily controlled by the field strength and exposure time, resulting in a wide range of rGO with different

conductivity/dispersibility features. The partially reduced GO (prGO) sheets with engineered conductivity/dispersibility are used to prepare aqueous composites with a redox-polymer for organic battery applications. Additonally, at higher potentials, Pt nanoparticles are released from the feeder electrodes and attached to rGO sheets. The sheets were used for catalyzing hydrogen evolution reaction with a performance comparable to bulk Pt.

1. Introduction

Since the discovery of graphene in 2004, this type of two-dimensional (2D) materials have become a cornerstone of contemporary materials science.[1-5] This is due to their unique mechanical, electrical, thermal, and optical properties, impacting research in different fields such as electronics, energy, biomedicine, and sensing.[6-11] Among suggested approaches for the preparation of graphene, the transformation of graphene oxide (GO) to reduced graphene oxide (rGO) is considered as a promising, commercially feasible technique.[12] GO is a carbon-based nanomaterial in the form of atomically thin 2D sheets, bearing oxygen functions including carboxyl, hydroxyl, or epoxy groups.[13, 14] In contrast to graphene, GO is well-solubilized in water and a wide range of organic solvents, thus allowing (i) facile fabrication of uniform films on different substrates and networks,[15, 16] and (ii) precise engineering of composite materials in solutions with molecular-level interactions.[17-20] Such properties place this 2D material in a unique position for different applications, particularly energy-related devices.[21] However, GO is electrically insulating and zero-band gap graphene is obtained only when sp^2 lattices are regenerated.

Several methods including chemical, thermal and electrochemical techniques have been suggested to transform GO into rGO and partially restore the structure and characteristics of graphene.[12] Electrochemical techniques often outperform other systems in terms of toxicity and energy consumption. Typically, a film of GO (or its composites) is initially deposited on

an electrode, followed by applying a reductive potential to trigger the GO → rGO transformation. This technique faces three serious limitations: (i) the efficient reduction is only possible if the GO film is moderately thin or highly porous; (ii) an efficient electrochemical reduction often causes significant changes in the morphology of the film, which could largely influence the electrochemical behaviour and the stability of the film; (iii) this method is limited to GO samples that are already deposited on the electrode and it is difficult to isolate the obtained rGO sheets.

Here, we demonstrate an alternative approach to reduce GO sheets dispersed in a 2D solution phase based on bipolar electrochemistry (BPE). This contact-less approach has already been successfully applied on single or double layers of graphene (80×70 mm^2, attached to a substrate), to precisely modify its peripheries by one or two different metals.[22] However, this system was limited to large graphene sheets deposited on a surface and cannot be used for reduction of GO micro/nanosheets.

In this contribution, we designed a novel BPE setup consisting of a quasi-2D reaction environment to benefit from the aforementioned advantages of electrochemical reduction systems, while avoiding the limitations. BPE, in contrast to conventional electrochemistry, is not using a classic working electrode (WE) that is connected to a power source. It is a wireless system, where the reaction occurs on the desired object (GO as the bipolar electrode in the current study), that is placed between two feeder electrodes without any direct contact with them (Fig. 1a). Upon application of an electric field, the conductive/semiconductive object gets polarized with respect to the surrounding solution, generating a polarization potential gradient along the length of the object.[23-26] The two ends of the object experience the highest cathodic/anodic polarization (with an opposite polarity compared to the feeder electrodes). The polarization potential that is established at the extremities of the object, *i.e.*

GO, is responsible for the reductive GO/rGO transformation, following a similar mechanism as for the conventional reduction of GO.

In the current study, the as-prepared rGO sheets are still well-dispersed in the solution. Notably, we have used a new setup based on a thin 2D reaction layer, in which the 2D bipolar electrodes are trapped in the freestanding layer. This is designed to overcome challenging limitations of conventional 3D BPE setups *i.e.* the precipitation and/or the random orientation of bipolar electrodes during the reaction and hence unequal and/or short exposure of bipolar electrodes to the desired potential gradient.[27-29] This issue is normally addressed by preparing highly viscous systems *e.g.*, gels, which is often limiting due to the difficulty of dispersing bipolar electrodes in the gel and their extraction after the reaction, as well as the difficulty of the incorporation of the desired salts (*e.g.* for metal deposition) into the gel structure.[27-29]

2. Methods

Materials: H_2SO_4, NaCl, KCl, Na_2HPO_4, KH_2PO_4 and glycerol were purchased from Sigma-Aldrich. Polyviologen (PV) was prepared following a method described in a previous study.[18] GO was prepared based on the Hofmann method.[30]

Reduction of GO via bipolar electrochemistry: A homemade quasi-2D bipolar electrochemical setup as shown in Fig. 1a with dimensions of 0.6×0.4×0.1 cm was built to prepare prGO and rGO. Two Pt wires (diameter: 0.25 mm) were used as feeder electrodes. In front of each feeder electrode, a membrane was placed to prevent a direct contact between the graphene sheets and the electrodes. Feeder electrodes were connected to a power source (Heinzinger PNC 10000-200 pos) *via* wrapping wires (Kynar). The GO solution was prepared by mixing 0.4 ml PBS buffer (pH: 7.4), containing 1.5 mg ml^{-1} GO, with 0.7 ml glycerol followed by 30 min mechanical mixing and 5 min sonication. 60 µl of the obtained solution

was suspended as a free-standing quasi-2D film between the two feeder electrodes in the bipolar setup using a micropipette.

X-ray diffraction (XRD): XRD patterns were acquired using a Bruker D8 Discoverer powder diffractometer (Bruker, Germany) in Bragg-Brentano parafocusing geometry and applying Cu K_α radiation (λ = 0.15418 nm, U = 40 kV, I =40 mA). The diffraction patterns were collected between 5^o and 90^o of 2θ with a step size of 0.020^o and the acquired data were evaluated using HighScore Plus 3.0e.

High-resolution transmission electron microscopy (HR-TEM): HR-TEM was performed with an EFTEM Jeol 2200 FS microscope (Jeol, Japan). A 200 keV acceleration voltage was used for measurement. Elemental maps were recorded with a SDD detector X-Max^N 80 TS (Oxford Instruments, England). All samples were put on a carbon TEM grid (Ted Pella Inc.) prior to the measurements.

X-ray photoelectron spectroscopy (XPS): XPS measurements were performed in an SPESC XPS spectrometer with Phoibos 150 hemispherical energy analyser (Specs, Germany) employing a monochromatic aluminum X-ray radiation source (1486.7 eV). Wide-scan surveys of all elements were performed with subsequent high-resolution scans of carbon (C 1s) and oxygen (O 1s). The samples were placed on a Si wafer. For elimination of the sample charging during measurement, an electron gun was utilized (1–5 V). All XPS survey spectra were afterwards analyzed by CasaXPS software.

SEM/EDX: SEM coupled with EDS mapping was performed with a Lyra3 GM Tescan microscope. The samples were coated on conductive carbon by drop-casting and drying at 50 ^{o}C for 1h. The measurement was performed using 20 kV acceleration voltage.

Electrical properties: The conductivity measurements were performed by drop-casting of 5 µl GO solution on interdigital microarray electrodes (dimension: 1cm × 0.5cm, featuring

separated 10 μm Pt bands deposited on it), followed by drying at 50 ºC for 3h. The resistance between electrodes was measured using a multimeter.

UV-Vis: The measurements were performed using Cary 100 UV-Visible Spectrophotometer. The samples were kept in a dark container between measurements.

Energy storage and conversion: The electrochemical measurements were performed using a Palmsens4 potentiostat interfaced with a computer with PSTrace software using a three-electrode system. A 3/1 PV/p(rGO) solution was prepared by mixing 0.2 ml of freshly sonicated (5 min) (p)rGO solution (containing 0.1 mg (p)rGO) with 0.8 ml of PV solution (containing 0.3 mg PV, without considering counterions). After mixing, the prGO composite was stirred for 10 min, while the rGO solution was sonicated for 1h. CV tests were performed using 0.1 KCl solution as an electrolyte, a Pt wire as a counter electrode (CE), Ag/AgCl as reference electrode (RE), and glassy carbon decorated with PV and PV composites as working electrode (WE). WEs were decorated by drop-casting the active materials and drying at 50 ºC for 1h. HER was performed using a three-electrode configuration with 0.5 M H_2SO_4 as the electrolyte (degassed with argon for 20 min before measurements), Ag/AgCl as RE, a graphite rod as CE, and a glassy carbon electrode decorated with GO and reduced GO as WE. WEs were prepared *via* drop-casting of the suspensions followed by drying at 50 ºC for 1h.

3. Results and Discussion

In the proposed 2D system (Fig. 1a), the reductive reaction on GO sheets as bipolar electrodes are occurring in an ultrathin aqueous layer positioned between two feeder electrodes. The degree of the reduction of GO and thus the conductivity of the resulting partially or totally reduced GO (prGO or rGO) sheets can be precisely controlled by changing the applied potential and the exposure time. In contrast to the conductivity, the dispersibility of the sheets

decreases when increasing the reduction state, due to the removal of the oxygen-containing functional groups (Fig. 1b). We have been able to synthesize prGO, which is still well-dispersed, but already provides sufficient electrical conductivity as a conductive filler in a composite with redox-active organic polymer (polyviologen), leading to a similar power density as with completely reduced rGO. Furthermore, it was observed that the rGO produced at high voltages contains an extremely low amount of platinum (Pt) nanoparticles (< 1%) released from the platinum feeder electrodes, which can be advantageously used for electrocatalytic reactions. rGO samples with high electrical conductivity, decorated with Pt, were used for studying hydrogen evolution reaction (HER). Remarkably, the electrodes with a C/O ratio ~ 6 showed an overpotential comparable to pure Pt metal (Fig. 1b). These different aspects are discussed one by one in more detail in the following sections.

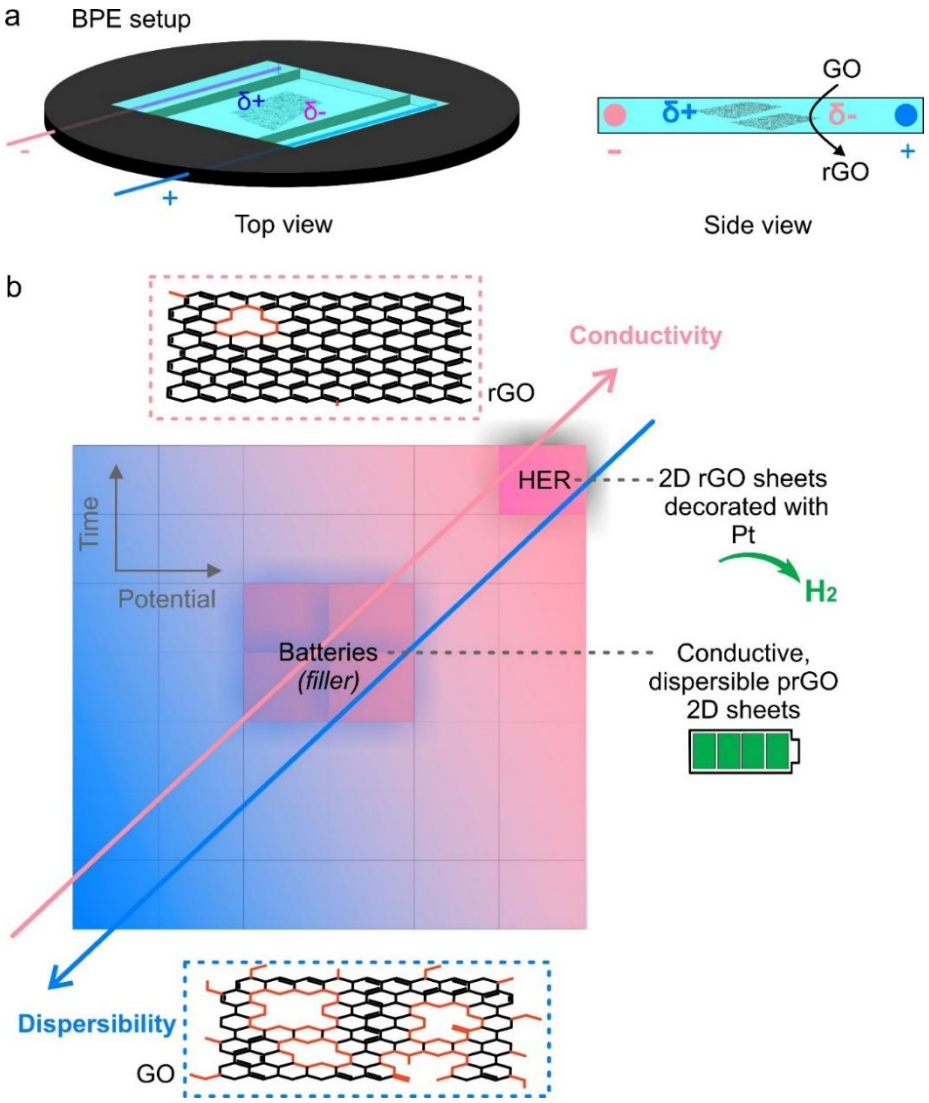

Fig. 1. a) Schematic overview of the bipolar electrochemical setup. Length: 0.6 cm, Width: 0.4 cm, Thickness: < 0.1 cm. b) Correlation between conductivity and dispersibility of (p)rGO with increasing time and potential of GO reduction. Partially reduced GO (prGO) can be used as dispersible conductive filler to facilitate composite preparation in the solution, while the highly reduced GO (rGO) is decorated with an extremely low amount of Pt (released from Pt feeder electrodes) that can be used for catalysis of electrochemical hydrogen evolution (HER).

3.1. GO → prGO → rGO transformation *via* bipolar electrochemistry

The wireless electrochemical reduction using a bipolar electrochemical setup (Fig. 1a) was performed with free-standing films of aqueous solutions containing GO by applying different potentials (10, 20, 40, 60, and 80V) for 4 min. The novel BPE set-up using a thin reaction space is suggested to better control the dispersibility, and conductivity of the sheets. In this setup, 2D sheets of graphene oxide are placed in a freestanding 2D water-based electrolyte film, which inhibits the precipitation or random orientation of the bipolar objects. Hence, the sheets are homogeneously treated with a constant polarisation potential during the reaction time. This allows a more precise control of the properties of the sheets by varying the potential and the reaction time. Two membranes were placed in front of the Pt feeder electrodes to inhibit direct connection between GO sheets and the electrodes during the experiment. The obtained (p)rGO was washed several times with water and then drop cast on an interdigitated electrode to measure their conductivity (Fig. 2a, -●- blue). A slight increase in the conductivity of the sheets was observed upon increasing the potential from 10 to 40 V, however, a jump in the conductivity of the sheets was observed at 60 V, which was further enhanced at 80 V. We have noticed that at lower concentrations of GO (<5 times, see experimental section), no GO → rGO transformation was observed. This is because the potential range applied in this work does not match the minimum potential necessary (~ 1 kV) to reduce individual small GO particles (5 – 10 μm) in the proposed setup. It should be noted that the current setup is designed to reduce the bypass current leading to a more energy efficient GO/rGO transformation, while improving the precipitation problem of the bipolar objects. However, a similar concept can be extrapolated to a more conventional setup if the applied potential and the composition of the electrolyte solution are adjusted.

The successful GO reduction in this study is attributed to the formation of larger colloids of GO as a result of the interconnection of GO sheets at higher concentrations. Their formation

is also related to the GO samples used in this work (prepared by the Hofmann method) with a low oxidation degree (32% oxygen content) and hence low solubility (20% precipitation after 10 min in the electrolyte solution).[30] Typically, BPE is performed in a highly viscous environment to avoid the rotation of bipolar objects and perform side selective reactions. However, we have chosen a different approach by performing reactions in a freestanding thin layer that is only viscous enough to be stable upon applying the potential, but not too viscous to avoid the free movement of particles. Hence, the bipolar objects are randomly moving in the plane of the liquid layer with an orientation parallel to the liquid film. This enables them to form dynamic 2D clusters. These dynamic clusters of GO have a size which allows establishing a polarization zone within the cluster that is large enough to put entire GO sheets, being located at the δ^- extremity of the cluster, on a sufficiently negative potential to reduce the oxygen functionalities. As the assembly is dynamic they can be replaced subsequently by not yet reduced GO sheets, until statistically all sheets have undergone a reduction. Reoxidation at the opposite extremity of the cluster is not occurring, because water oxidation is easier than oxidation of graphene.

The photos of the GO solutions reduced at different potentials are presented in Fig. 2b. The color of the solution changes from light brown to dark brown and finally black indicating the transformation of GO to prGO and finally rGO. Note that each of these solutions is the mixture of 10 individual experiments and the reported resistances are average values.

As a control experiment, hydroquinone (HQ) was added to the GO solution and a similar analysis was performed (Fig. 2a, -■- red). It is expected that the addition of this redox-active organic molecule facilitates GO reduction because HQ has a lower oxidation potential in comparison to water.[31] In this case, the resistance values and the corresponding color already change at 10 V, due to the lower required driving force.

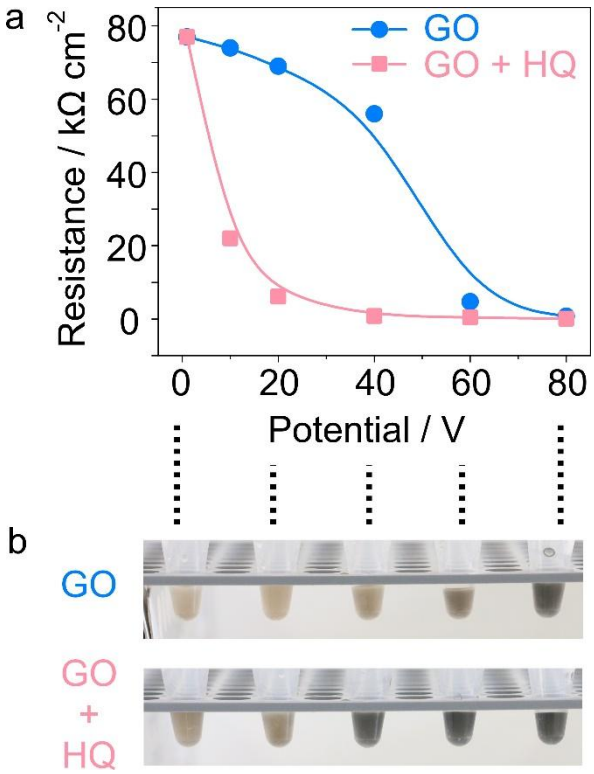

Fig. 2. Wireless reduction of GO. a) Resistance of GO synthesized at different potentials (10, 20, 40, 60, 80V) in the absence (blue, -●-) and in the presence (red, -■-) of HQ measured by drop-casting of the solution on interdigitated electrodes. b) The corresponding photos of GO solutions synthesized at different potentials. Each resistance value and solution is the average of 10 individual experiments.

3.2. Structural analysis

The crystalline structure of the GO sample before, during (at 40 V, *i.e.*, prGO), and after electrochemical reduction (at 100 V, *i.e.*, rGO) was measured *via* X-ray powder diffraction (XRD) analysis (Fig. 3a). GO shows the characteristic carbon peak (001) at $2\theta = 10.9°$ corresponding to a d-spacing of 0.81 nm, while prGO and rGO show broad peaks due to deterioration of crystallinity of GO sheets with higher values, indicating a smaller layer distance after the GO/rGO transformation due to the removal of functional oxygen groups.[18] In addition, high-resolution transmission electron microscopy (HR-TEM) and

selected area electron diffraction (SAED) were performed on a typical lacey carbon substrate to characterize the crystallinity of a representative selection of the obtained sheets (Fig. 3b and S1). The HR-TEM image and energy dispersive X-ray spectroscopy (EDX) map of rGO appears to be highly electron transparent. The sheets are slightly wrinkled and counting the periodic stripped edges of sheets confirmed < 3 layers of rGO partially covering each other.[32] The SAED pattern (Fig. 3b, inset) shows a hexagonal array of diffraction peaks, in agreement with the crystal structure of graphene sheets. The spots are labeled *via* (hkl) Miller–Bravais notation.[33] X-ray photoelectron spectroscopy (XPS) of GO at different oxidation states was performed to obtain more details about the elimination of oxygen-containing functional groups during the wireless electrochemical reduction process. As shown in Fig. 3c, the C 1s spectrum of GO exhibits peaks at 284.5 (C=C), 285.4 (C-C), 286.3 (C-O), 287.9 (C=O), and 290.9 (O-C=O) eV, attributed to the sp^2 carbon, sp^3 carbon, the epoxy, carbonyl, and carboxyl functional groups, respectively. After electrochemical treatment of the sample at 40 V for 4 min (prGO), the peak intensity of oxygen-containing functional groups significantly decreases, while a higher intensity of sp^3 carbon compared to sp^2 carbon is still observed, indicating removal of oxygen groups and uncompleted regeneration of sp^2 carbons. This is attributed to the removal of the oxygen-containing functional groups and a partial regeneration of the conjugated π system. Applying a higher potential, *i.e.* 100 V (rGO), results in a significant enhancement of the sp^2 carbon (C=C) peak, in comparison to all other peaks, indicating an efficient GO → rGO transformation.[34]

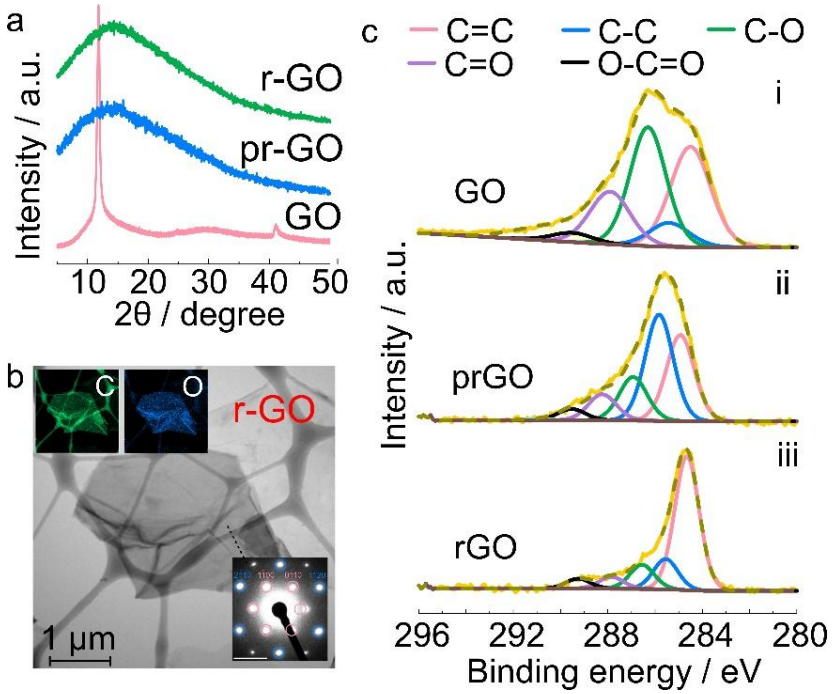

Fig. 3. Structural analysis. a) XRD patterns of GO, prGO, and rGO. b) HR-TEM of rGO and its corresponding EDX map (carbon and oxygen) and SAED pattern as an inset image. c) XPS curves of (i) pristine GO, (ii) prGO (40V, 4 min) and (iii) rGO (100V, 4 min).

3.3. Conductivity and dispersibility

The conductivity and the carbon/oxygen (C/O) ratio of GO samples after electrochemical treatments at different potentials (20, 40, 60 80, 100 V) and treatment times (1, 2 4 min) were measured (Fig. 4). The resistance and C/O ratio values are the average of 10 independent experiments. The GO suspensions were washed several times with distilled water before all analyses. As shown in Fig. 4a, applying a potential decreases the resistance of the samples, which is in agreement with the gradual color changes from brown to black as a function of the applied potential (Fig. S2). The resistance of samples significantly decreases at 40 V, particularly for the 4 min experiment, which appears to be a critical potential for the proposed wireless reduction of GO *via* bipolar electrochemistry. Such intermediate phase shifts in the

conductivity are also observed in other reduction mechanisms, which is attributed to the growth of enough graphitic domains to allow efficient percolative electronic transport.[35] At higher potentials (60, 80, and 100 V), even lower resistances down to 7 Ω cm^{-2} (4 min, 100V) were recorded, however, the relative resistance changes beyond 40 V were smaller. In order to better understand the origin of these changes, the ratio between the atomic contents of carbon and oxygen in samples produced at different potentials was measured *via* SEM/EDX (Fig. S3-S4). In samples with 1 or 2 min treatments, a steady increase of the C/O ratio with a small jump at 80 V is observed, while in the case of 4 min treatment, a much higher jump is recorded (Fig. 4b). This C/O ratio phase shift, which occurs at a higher potential than the conductivity phase shift is attributed to the massive removal of oxygen-containing functional groups.[35] Remarkably, the final C/O ratio in the samples with 4 min electrochemical treatment (Fig. 4b) is significantly higher than for other samples, which is in agreement with their conductivity. Note that, while other GO reduction methods, *e.g.* thermal treatment, might result in C/O ratios > 8 (reduction at > 500 ºC), the electrochemical approach is more economical in terms of energy efficiency and the electrical conductivity achieved *via* both systems is comparable even if the C/O ratios obtained with the proposed method are lower [36]. As for the purpose of this work the critical factor is the electrical conductivity, the electrochemical approach appears to be a satisfying alternative.

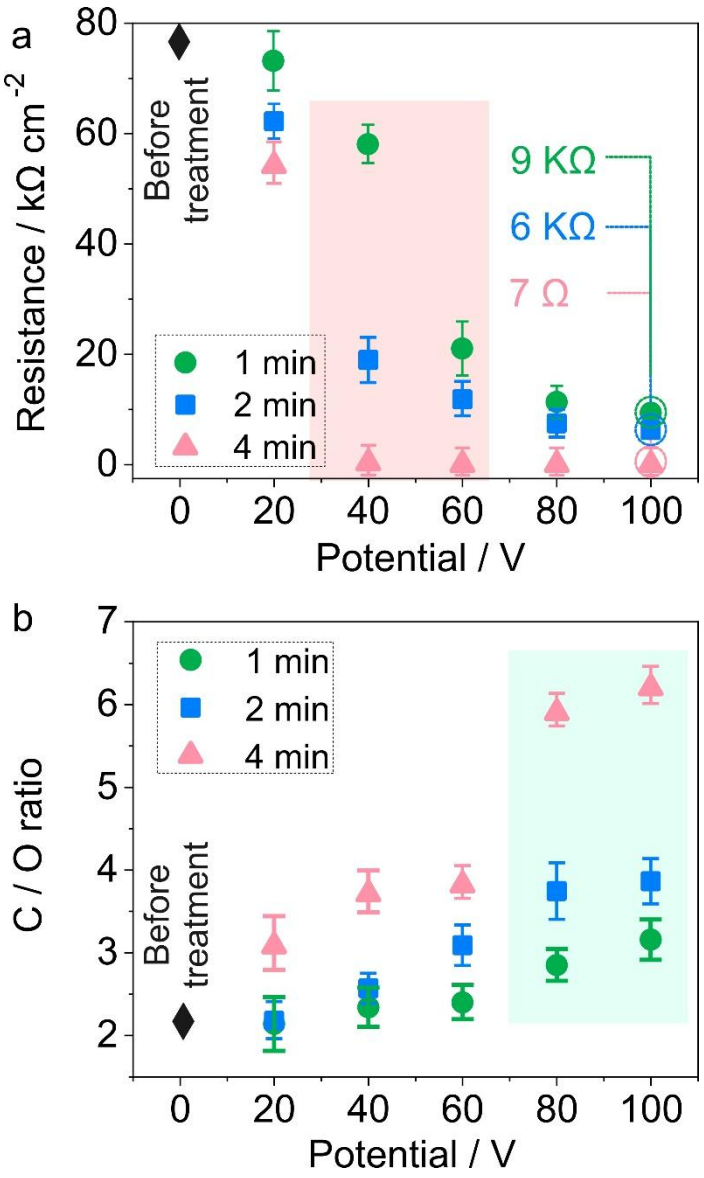

Fig. 4. The resistance and the carbon content of samples during the GO → prGO → rGO transformation. a) Resistance (kΩ cm^{-2}) of GO and the electrochemically treated samples at different potentials (20, 40, 60 80, 100 V) obtained with samples deposited on interdigitated electrodes. The phase shift in the resistance of the samples is highlighted. b) EDX measurements of the C/O ratio of GO samples obtained by applying for 1, 2, and 4 min different potentials as in (a). The phase shift in the C/O ratio of the samples is highlighted. All values are the average of 10 independent experiments.

Subsequently, the dispersibility of the obtained prGO and rGO in an aqueous solution is compared with the original GO suspension. This is important regarding the preparation of hierarchical nanostructures and macroscopic composite materials *via* supramolecular self-assembly mechanisms to generate new properties and functionalities for various technological applications such as (opto)electronics, catalysis and energy conversion.[19, 37] The stability of samples in distilled water is evaluated by their UV adsorption at different time intervals (Fig. S5). As shown in Fig. 5a, pristine GO solutions showed the lowest precipitation after 48 h, compared to GO solutions that were electrochemically treated for 4 min (see Fig. S6 for 1 and 2 min treatments). It is evident that increasing the potential results in the formation of prGO and rGO suspensions that are less stable in water. This is explained by the removal of their oxygen-containing functional groups (Fig. 3), resulting in lower solubility in polar solvents.[17, 38] The dispersibility is also studied as a function of the duration of the electrochemical treatment at different potentials (Fig. 5b, and S5). While in all cases lower dispersibility is observed for higher potentials, longer treatments *i.e.*, 4 min resulted in even lower dispersibility. Notably, a considerable change in the dispersibility of prGO was observed at 40 V (Fig. 5b, red), which correlates well with the enhanced conductivity observed at the same potential (Fig. 4a, red).

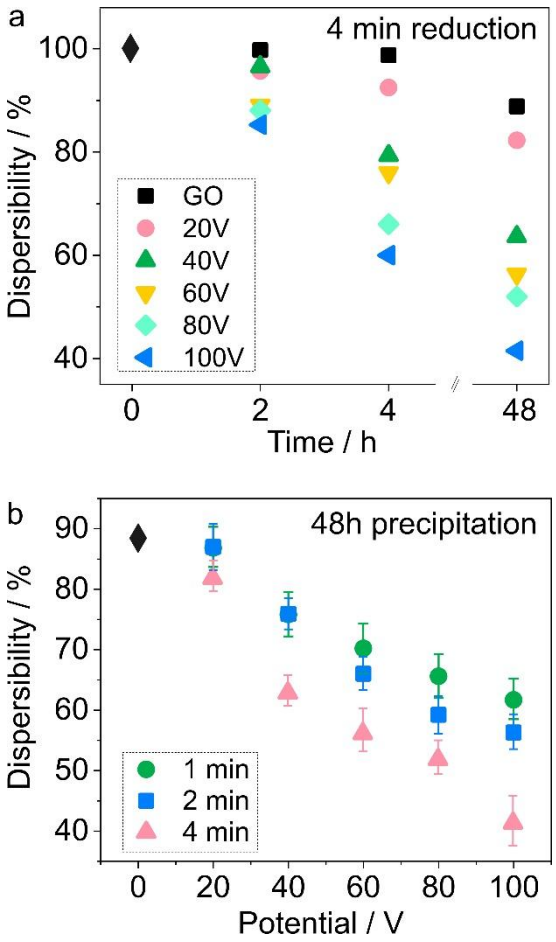

Fig. 5. Dispersibility for different reduced states. a) Dispersibility of pristine GO and samples electrochemically reduced for 4 min at potentials of 20, 40, 60, 80 and 100 V, estimated from their UV absorption with standard deviations of 4.3, 5.6, 13.9, 13.5, 14.9, and 18.9, respectively; the samples were washed and sonicated before this measurement. b) Dispersibility after 48h of pristine GO electrochemically treated for 1, 2, and 4 min at different potentials (20, 40, 60. 80 and 100 V).

3.4. Applications

3.4.1. Energy storage

Single sheets of graphene are ideal fillers to provide both electrical and ionic conductivity in battery materials.[39] This is due to graphene's high electrical conductivity and the lower

amount of required conductive fillers if single sheets of graphene are efficiently distributed among active materials.[40] However, the low solubility and immediate restacking of graphene sheets after the exfoliation process make them impractical for large-scale applications. Hence, in many studies, GO is initially used as the filler, which is followed by a thermal GO → rGO transformation step of the final electrode. Nevertheless, this is only possible if the active material can tolerate temperatures above 350 °C.[41] Electrochemical methods are also suggested to reduce GO at the surface of electrodes *via* applying cathodic potentials.[42] Nonetheless, GO is electrically insulating, and electrochemical reduction is only efficient for thin layers. In the current study, composites of a redox-active organic polymer *i.e.*, polyviologen (PV) and prGO (reduced at 40V) or rGO (reduced at 100V) are prepared *via* mixing of their aqueous solutions with a PV/(p)rGO ratio of 3. PV is a dicationic polymer (PV^{++}), which can be reversibly reduced to the radical cation state at cathodic potentials (Fig. 6a). As shown in our previous studies, a self-assembly between PV^{++} and fillers (GO/rGO) *via* electrostatic and/or π-π interaction is expected.[18] The obtained composites are drop cast on current collectors and the electrodes are charged and discharged at different scan rates while discharge capacities are recorded. Cyclic voltammetry (CV) curves at 20 mV s^{-1}, exhibiting a redox signal at ~ -0.3V (vs. Ag/AgCl) are shown in Fig. 6b (see other scan rates in Fig. S7). The reduction current has a lower peak value, but the peak is very broad, while the oxidation current exhibits a higher and sharper peak. However, integration of both peaks leads to very similar values, indicating that the charge transfer process is completely reversible. The areal capacity of the PV alone or PV composite with GO is significantly lower than the PV composites with electrically conductive prGO and rGO. Remarkably, the capacity of composites in the presence of prGO or rGO are very similar. This demonstrates the efficiency of prGO to provide enough electrical conductivity in the battery materials, while this filler is much more dispersible in aqueous solutions compared to rGO

samples. This becomes even more evident when taking into account the easy composite preparation procedure by simple mixing of prGO and PV, while the rGO composite needs a harsh time-consuming sonication shortly before experiments for a similar performance. A comparable trend in the behaviour of the composites is observed at different scan rates (Fig. 6c).

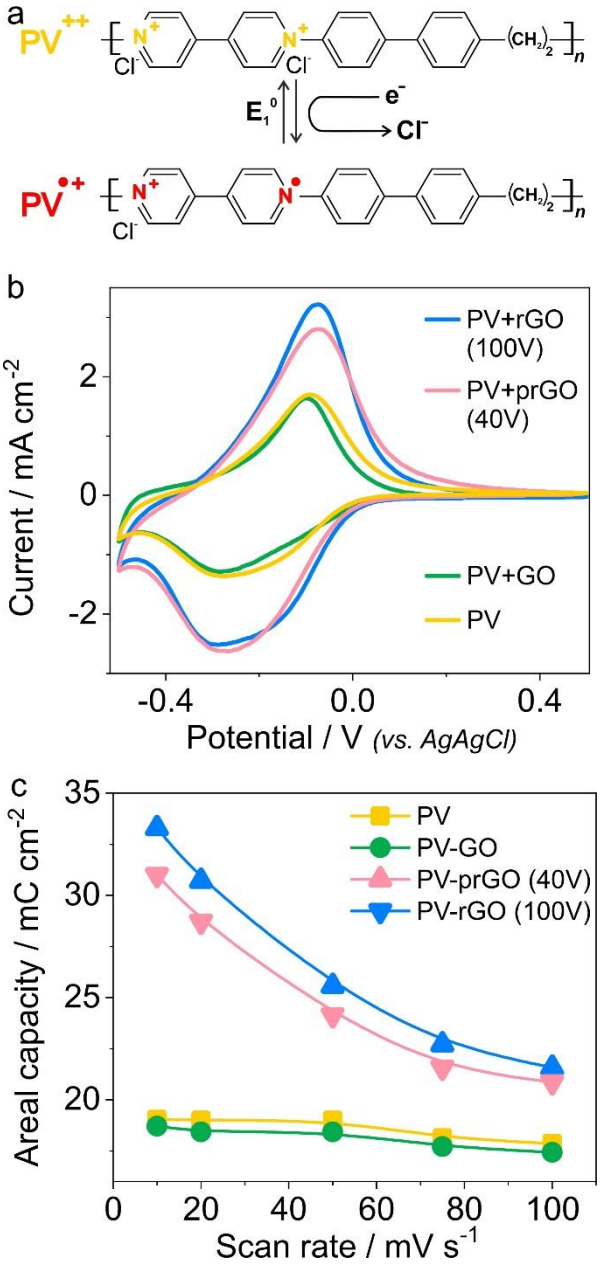

Fig. 6. The energy storage performance of PV composites. a) Reversible redox reactions of PV ($PV^{++} \leftrightarrow PV^{\bullet+}$). b) CV curves of PV, PV-GO, PV-prGO (40V), and PV-rGO (100V) at 20 mV cm^{-2}. c) The areal capacity (mC cm^{-2}) of PV, PV-GO, PV-prGO (40V), and PV-rGO (100V) at different scan rates (10, 20, 50, 75, and 100 mV s^{-1}) obtained from the discharge curves of their CVs. Ag/AgCl reference electrode, Pt wire counter electrode, glassy carbon decorated with PV, and PV composites as the working electrode.

3.4.2. Electrocatalysis

Pt is widely used in electrolyzers for water splitting due to its excellent catalytic characteristics, however, the high price and limited resources of Pt are seriously limiting factors. Various materials *e.g.*, transition metal oxides are proposed to replace Pt, however, these materials can barely provide comparable activities and are often produced through expensive and time-consuming procedures. An attractive alternative method could be to elaborate electrodes using extremely low quantities of Pt while keeping its electrocatalytic performance. The wireless electrochemical reduction of GO proposed in this study involves two Pt feeder electrodes. It should be noted that in principle these Pt electrodes can be replaced by other appropriate materials such as carbon. However, in the present work we used Pt on purpose in order to verify whether it might be possible to trigger the release of extremely small quantities of this noble metal from the feeder electrodes, which then can act as catalytically active modifiers of the rGO sheets. HR-TEM of rGO reduced at 100 V indicates the presence of micro/nano-sized Pt particles (down to 0.6 wt%), mapped by the corresponding EDX analysis (Fig. 7a and S8-S9). The obtained rGO/Pt samples were washed with distilled water and drop cast on a glassy carbon current collector and their performance for HER was assessed in 0.5 M H_2SO_4. The linear sweep voltammetry (LSV) curves of rGO,

produced at different potentials (20-100V), are compared with the LSV of pristine GO and a bulk Pt electrode (Fig. 7b). It should be noted that the currents are normalized with respect to the geometric surface area of the electrodes. Overpotential values at a current density of 10 mA cm^{-2} are compared for the different samples (Fig. 7c). Significantly lower overpotential values were recorded for samples that were synthesized at higher potentials in the bipolar modification experiments. However, a significant jump in the overpotential value was observed at 80 V. This is attributed to (i) the adsorption of Pt particles on the surface of rGO sheets, detached from feeder electrodes at higher potentials and (ii) the high electrical conductivity of the rGO sheets and thus of the final electrode. Notably, the performance of the rGO with homogenously distributed Pt particles (Fig. S9) that are produced at 80 and 100V have overpotential values of 161 and 94 mV (at 10 mA cm^{-2}), respectively, which are comparable to those measured for a bulk Pt electrode (63.5 mV). This indicates an excellent performance of these electrodes, even in the presence of only 0.6 wt % of Pt, which is an order of magnitude lower than some literature values.[43] Fine tuning of the Pt release from the feeder electrodes might even allow a further decrease of the relative Pt content, while keeping a similar catalytic performance. In order to evaluate the stability of the rGO/Pt film, a chronopotentiometry experiment at 10 mA cm^{-2} was performed for 2000 seconds (Fig. 7d). Despite minor fluctuations, no significant degradation was observed at this time scale.

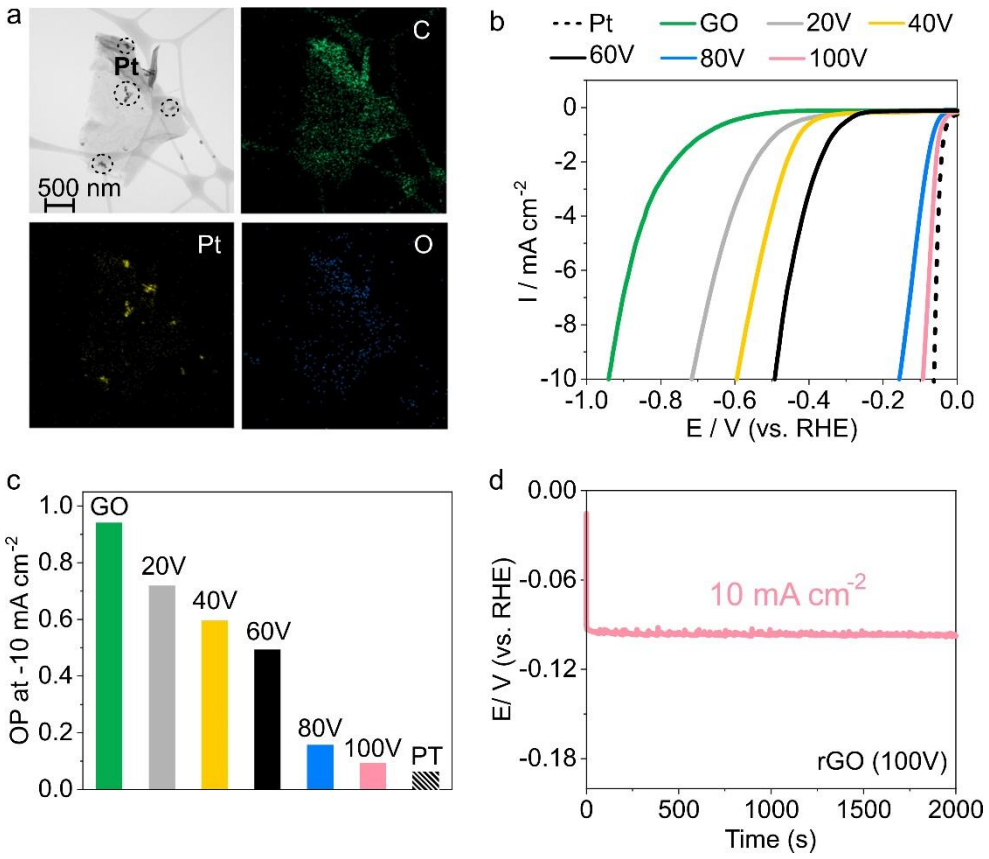

Fig. 7. The hydrogen evolution performance of rGO decorated with Pt. a) HR-TEM of thin sheets of rGO (100V) with corresponding EDX maps of carbon, platinum, and oxygen. b) LSV curves of GO, rGO decorated with Pt, and a Pt wire as a reference sample, at a scan rate of 2 mV s^{-1}. c) Overpotential values at a current density of -10 mA cm^{-2}. d) Chronopotentiometry of rGO decorated with 0.6 wt% Pt (GO reduction at 100V for 4 min) at a current density of 10 mA cm^{-2}.

4. Conclusions

We have prepared rGO sheets with different oxidation states using an original BPE set-up based on a quasi-2D reaction space. This system allows overcoming typical limitations of the conventional 3D BPE setups, such as the precipitation and/or the random rotation of the plane

of bipolar electrodes with respect to the electric field lines during the reaction and hence unequal and/or short exposure of bipolar electrodes to the desired polarization potential. The approach results in a single-step preparation – directly in an aqueous solution without any contact with the feeder electrodes– of highly conductive yet dispersible sheets without the presence of any surfactant. Moreover, the proposed 2D setup enables a precise control of the degree of oxidation, and thus a fine-tuning of several physico-chemical properties of the sheets, by simply changing the electric field strength and reaction time. This mild and green approach doesn't require any toxic ingredients and produces high-quality (p)rGO sheets with adjustable electrical and chemical properties in a very short time (< 4 min) using a simple setup. As a proof-of-concepts, we have demonstrated the tunable performance of prGO sheets by using them as conductive fillers for organic batteries, and as catalysts for HER. Notably, as prepared prGO sheets, in contrast to typical carbon-based conductive fillers, are well-dispersed in aqueous solution, thus allowing a facile preparation of composites with organic redox polymers, having an energy storage performance comparable to highly reduced rGO. Regarding HER measurements, Pt/rGO sheets with very low Pt loading (< 1 wt%) could be synthesized in a set of proof-of-principle experiments at high potentials, exhibiting an HER activity comparable to the one of pure Pt metal in terms of overpotential and current density. Such experiments might be pushed further in the future to reach still a similar catalytic performance, but with even lower percentages of metal. The proposed straightforward synthesis process therefore opens up promising perspectives for the controlled elaboration of designer nano- and micromaterials with various functionalities. Further expansion of such systems based on wireless electrochemistry might result in novel approaches for the preparation of graphene-based composites.

Credit author contribution statement

The manuscript has been read and approved by all named authors.

Declaration of competing interest

There are no conflicts to declare.

Acknowledgements

The work has been funded by the European Research Council (ERC) under the European Union's Horizon 2020 research and innovation program (grant agreement n° 741251, ERC Advanced grant ELECTRA). Z.S. was supported by Czech Science Foundation (GACR No. 20-16124J).

Appendix A. Supplementary data

Supplementary data to this article can be found online

References

[1] K.S. Novoselov, A.K. Geim, S.V. Morozov, D. Jiang, Y. Zhang, S.V. Dubonos et al., Electric Field Effect in Atomically Thin Carbon Films, Science 306(5696) (2004) 666. http://science.sciencemag.org/content/306/5696/666.abstract
[2] J.C. Meyer, A.K. Geim, M.I. Katsnelson, K.S. Novoselov, T.J. Booth, S. Roth, The structure of suspended graphene sheets, Nature 446(7131) (2007) 60-63. https://doi.org/10.1038/nature05545
[3] H. Huang, H. Shi, P. Das, J. Qin, Y. Li, X. Wang et al. , The Chemistry and Promising Applications of Graphene and Porous Graphene Materials, Advanced Functional Materials 30(41) (2020) 1909035. https://doi.org/10.1002/adfm.201909035
[4] S.M. Beladi-Mousavi, A.M. Pourrahimi, Z. Sofer, M. Pumera, Atomically Thin 2D-Arsenene by Liquid-Phased Exfoliation: Toward Selective Vapor Sensing, Advanced Functional Materials 29(5) (2019) 1807004. https://doi.org/10.1002/adfm.201807004
[5] X. Li, X. Yin, S. Liang, M. Li, L. Cheng, L. Zhang, 2D carbide MXene Ti2CTX as a novel high-performance electromagnetic interference shielding material, Carbon 146 (2019) 210-217. https://www.sciencedirect.com/science/article/pii/S0008622319301162
[6] M.D. Stoller, S. Park, Y. Zhu, J. An, R.S. Ruoff, Graphene-Based Ultracapacitors, Nano Letters 8(10) (2008) 3498-3502. https://doi.org/10.1021/nl802558y

[7] Q. Ma, C.H. Lui, J.C.W. Song, Y. Lin, J.F. Kong, Y. Cao et al. , Giant intrinsic photoresponse in pristine graphene, Nature Nanotechnology 14(2) (2019) 145-150. https://doi.org/10.1038/s41565-018-0323-8
[8] G. Reina, J.M. González-Domínguez, A. Criado, E. Vázquez, A. Bianco, M. Prato, Promises, facts and challenges for graphene in biomedical applications, Chemical Society Reviews 46(15) (2017) 4400-4416. http://dx.doi.org/10.1039/C7CS00363C
[9] S. Banerjee, J. Wilson, J. Shim, M. Shankla, E.A. Corbin, A. Aksimentiev et al. , Slowing DNA Transport Using Graphene–DNA Interactions, Advanced Functional Materials 25(6) (2015) 936-946. https://doi.org/10.1002/adfm.201403719
[10] M. Khan, M.N. Tahir, S.F. Adil, H.U. Khan, M.R.H. Siddiqui, A.A. Al-warthan et al., Graphene based metal and metal oxide nanocomposites: synthesis, properties and their applications, Journal of Materials Chemistry A 3(37) (2015) 18753-18808. http://dx.doi.org/10.1039/C5TA02240A
[11] T.H. Nguyen, D. Yang, B. Zhu, H. Lin, T. Ma, B. Jia, Doping mechanism directed graphene applications for energy conversion and storage, Journal of Materials Chemistry A 9(12) (2021) 7366-7395. http://dx.doi.org/10.1039/D0TA11939C
[12] S. Pei, H.-M. Cheng, The reduction of graphene oxide, Carbon 50(9) (2012) 3210-3228. https://www.sciencedirect.com/science/article/pii/S0008622311008967
[13] D.R. Dreyer, A.D. Todd, C.W. Bielawski, Harnessing the chemistry of graphene oxide, Chemical Society Reviews 43(15) (2014) 5288-5301. http://dx.doi.org/10.1039/C4CS00060A
[14] A. Bonanni, A. Ambrosi, M. Pumera, On Oxygen-Containing Groups in Chemically Modified Graphenes, Chemistry – A European Journal 18(15) (2012) 4541-4548. https://doi.org/10.1002/chem.201104003
[15] Y. Zhu, D.K. James, J.M. Tour, New Routes to Graphene, Graphene Oxide and Their Related Applications, Advanced Materials 24(36) (2012) 4924-4955. https://doi.org/10.1002/adma.201202321
[16] Y. Zhu, S. Murali, W. Cai, X. Li, J.W. Suk, J.R. Potts et al., Graphene and Graphene Oxide: Synthesis, Properties, and Applications, Advanced Materials 22(35) (2010) 3906-3924. https://doi.org/10.1002/adma.201001068
[17] S.M. Beladi-Mousavi, S. Sadaf, A.-K. Hennecke, J. Klein, A.M. Mahmood, C. Rüttiger, et al. , The Metallocene Battery: Ultrafast Electron Transfer Self Exchange Rate Accompanied by a Harmonic Height Breathing, Angewandte Chemie International Edition 60(24) (2021) 13554-13558. https://doi.org/10.1002/anie.202100174
[18] S.M. Beladi-Mousavi, S. Sadaf, A.M. Mahmood, L. Walder, High Performance Poly(viologen)–Graphene Nanocomposite Battery Materials with Puff Paste Architecture, ACS Nano 11(9) (2017) 8730-8740. https://doi.org/10.1021/acsnano.7b02310
[19] S.M. Beladi-Mousavi, S. Sadaf, L. Walder, M. Gallei, C. Rüttiger, S. Eigler et al. , Poly(vinylferrocene)–Reduced Graphene Oxide as a High Power/High Capacity Cathodic Battery Material, Advanced Energy Materials 6(12) (2016) 1600108. https://doi.org/10.1002/aenm.201600108
[20] A. Ambrosi, C.K. Chua, N.M. Latiff, A.H. Loo, C.H.A. Wong, A.Y.S. Eng, et al. , Graphene and its electrochemistry – an update, Chemical Society Reviews 45(9) (2016) 2458-2493. http://dx.doi.org/10.1039/C6CS00136J
[21] J.G. Radich, P.V. Kamat, Origin of Reduced Graphene Oxide Enhancements in Electrochemical Energy Storage, ACS Catalysis 2(5) (2012) 807-816. https://doi.org/10.1021/cs3001286
[22] L. Zuccaro, A. Kuhn, M. Konuma, H.K. Yu, K. Kern, K. Balasubramanian, Selective Functionalization of Graphene Peripheries by using Bipolar Electrochemistry, ChemElectroChem 3(3) (2016) 372-377. https://doi.org/10.1002/celc.201500461
[23] L. Bouffier, D. Zigah, N. Sojic, A. Kuhn, Bipolar (Bio)electroanalysis, Annual Review of Analytical Chemistry 14(1) (2021) 65-86. https://doi.org/10.1146/annurev-anchem-090820-093307
[24] S.E. Fosdick, K.N. Knust, K. Scida, R.M. Crooks, Bipolar Electrochemistry, Angewandte Chemie International Edition 52(40) (2013) 10438-10456. https://doi.org/10.1002/anie.201300947

[25] L. Koefoed, S.U. Pedersen, K. Daasbjerg, Bipolar electrochemistry—A wireless approach for electrode reactions, Current Opinion in Electrochemistry 2(1) (2017) 13-17. https://www.sciencedirect.com/science/article/pii/S2451910316300473
[26] N. Shida, Y. Zhou, S. Inagi, Bipolar Electrochemistry: A Powerful Tool for Electrifying Functional Material Synthesis, Accounts of Chemical Research 52(9) (2019) 2598-2608. https://doi.org/10.1021/acs.accounts.9b00337
[27] J. Roche, G. Loget, D. Zigah, Z. Fattah, B. Goudeau, S. Arbault et al, Straight-forward synthesis of ringed particles, Chemical Science 5(5) (2014) 1961-1966. http://dx.doi.org/10.1039/C3SC53329H
[28] G. Loget, J. Roche, A. Kuhn, True Bulk Synthesis of Janus Objects by Bipolar Electrochemistry, Advanced Materials 24(37) (2012) 5111-5116. https://doi.org/10.1002/adma.201201623
[29] M. Sentic, S. Arbault, L. Bouffier, D. Manojlovic, A. Kuhn, N. Sojic, 3D electrogenerated chemiluminescence: from surface-confined reactions to bulk emission, Chemical Science 6(8) (2015) 4433-4437. http://dx.doi.org/10.1039/C5SC01530H
[30] U. Hofmann, A. Frenzel, Die Reduktion von Graphitoxyd mit Schwefelwasserstoff, Kolloid-Zeitschrift 68(2) (1934) 149-151. https://doi.org/10.1007/BF01451376
[31] G. Loget, A. Kuhn, Electric field-induced chemical locomotion of conducting objects, Nature Communications 2(1) (2011) 535. https://doi.org/10.1038/ncomms1550
[32] R. Navik, Y. Gai, W. Wang, Y. Zhao, Curcumin-assisted ultrasound exfoliation of graphite to graphene in ethanol, Ultrasonics Sonochemistry 48 (2018) 96-102. https://www.sciencedirect.com/science/article/pii/S1350417718300555
[33] N.R. Wilson, P.A. Pandey, R. Beanland, R.J. Young, I.A. Kinloch, L. Gong et al. , Graphene Oxide: Structural Analysis and Application as a Highly Transparent Support for Electron Microscopy, ACS Nano 3(9) (2009) 2547-2556. https://doi.org/10.1021/nn900694t
[34] S. Park, J. An, I. Jung, R.D. Piner, S.J. An, X. Li et al. , Colloidal Suspensions of Highly Reduced Graphene Oxide in a Wide Variety of Organic Solvents, Nano Letters 9(4) (2009) 1593-1597. https://doi.org/10.1021/nl803798y
[35] A. Lipatov, M.J.F. Guinel, D.S. Muratov, V.O. Vanyushin, P.M. Wilson, A. Kolmakov et al. , Low-temperature thermal reduction of graphene oxide: In situ correlative structural, thermal desorption, and electrical transport measurements, Applied Physics Letters 112(5) (2018) 053103. https://doi.org/10.1063/1.4996337
[36] S. Pei, H.-M. Cheng, The reduction of graphene oxide, Carbon 50(9) (2012) 3210. https://doi.org/10.1016/j.carbon.2011.11.010
[37] Z. Yuan, X. Xiao, J. Li, Z. Zhao, D. Yu, Q. Li, Self-Assembled Graphene-Based Architectures and Their Applications, Advanced Science 5(2) (2018) 1700626. https://doi.org/10.1002/advs.201700626
[38] Y. Shao, J. Wang, M. Engelhard, C. Wang, Y. Lin, Facile and controllable electrochemical reduction of graphene oxide and its applications, Journal of Materials Chemistry 20(4) (2010) 743-748. http://dx.doi.org/10.1039/B917975E
[39] Z. Ju, X. Zhang, S.T. King, C.D. Quilty, Y. Zhu, K.J. Takeuchi et al. , Unveiling the dimensionality effect of conductive fillers in thick battery electrodes for high-energy storage systems, Applied Physics Reviews 7(4) (2020) 041405. https://doi.org/10.1063/5.0024123
[40] Z. Song, T. Xu, M.L. Gordin, Y.-B. Jiang, I.-T. Bae, Q. Xiao et al. , Polymer–Graphene Nanocomposites as Ultrafast-Charge and -Discharge Cathodes for Rechargeable Lithium Batteries, Nano Letters 12(5) (2012) 2205-2211. https://doi.org/10.1021/nl2039666
[41] I. Sengupta, S. Chakraborty, M. Talukdar, S.K. Pal, S. Chakraborty, Thermal reduction of graphene oxide: How temperature influences purity, Journal of Materials Research 33(23) (2018) 4113-4122. https://doi.org/10.1557/jmr.2018.338
[42] A. Viinikanoja, Z. Wang, J. Kauppila, C. Kvarnström, Electrochemical reduction of graphene oxide and its in situ spectroelectrochemical characterization, Physical Chemistry Chemical Physics 14(40) (2012) 14003-14009. http://dx.doi.org/10.1039/C2CP42253K
[43] M. P. Browne, F. Novotný, D. Bousa, Z. Sofer, M. Pumera, Flexible Pt/Graphene Foil Containing only 6.6 wt % of Pt has a Comparable Hydrogen Evolution Reaction Performance to Platinum Metal,

ACS Sustainable Chem. Eng. 7(13) (2019) 11721–11727.
https://doi.org/10.1021/acssuschemeng.9b01876